

## RESEARCH ARTICLE

10.1029/2017JD028242

## Key Points:

- High sulfate and low aerosol pH promote heterogeneous reactions of IEPOX, which favor isoprene SOA formation via the HO<sub>2</sub> channel
- High temperatures suppress the production of hydroxymethyl-methyl- $\alpha$ -lactone, thus limiting isoprene SOA formation via the NO/NO<sub>2</sub>-channel
- Controlling SO<sub>2</sub> emission could significantly reduce iSOA formation

## Supporting Information:

- Supporting Information S1

## Correspondence to:

X. Ding,  
xiangd@gig.ac.cn

## Citation:

He, Q.-F., Ding, X., Fu, X.-X., Zhang, Y.-Q., Wang, J.-Q., Liu, Y.-X., et al. (2018). Secondary organic aerosol formation from isoprene epoxides in the Pearl River Delta, South China: IEPOX- and HMML-derived tracers. *Journal of Geophysical Research: Atmospheres*, 123, 6999–7012. <https://doi.org/10.1029/2017JD028242>






Received 16 JAN 2018

Accepted 12 JUN 2018

Accepted article online 20 JUN 2018

Published online 7 JUL 2018

## Secondary Organic Aerosol Formation From Isoprene Epoxides in the Pearl River Delta, South China: IEPOX- and HMML-Derived Tracers

Quan-Fu He<sup>1,2</sup> , Xiang Ding<sup>1</sup> , Xiao-Xin Fu<sup>3</sup>, Yu-Qing Zhang<sup>1,4</sup>, Jun-Qi Wang<sup>1,4</sup>, Ye-Xin Liu<sup>5</sup>, Ming-Jin Tang<sup>1</sup> , Xin-Ming Wang<sup>1,6</sup> , and Yinon Rudich<sup>7</sup> 

<sup>1</sup>State Key Laboratory of Organic Geochemistry and Guangdong Provincial Key Laboratory of Environmental Protection and Resources Utilization, Guangzhou Institute of Geochemistry, Chinese Academy of Sciences, Guangzhou, China, <sup>2</sup>Now at Department of Earth and Planetary Sciences, Weizmann Institute of Science, Rehovot, Israel, <sup>3</sup>Southwest University of Science and Technology, Mianyang, China, <sup>4</sup>University of Chinese Academy of Sciences, Beijing, China, <sup>5</sup>Guangzhou Environmental Monitoring Center, Guangzhou, China, <sup>6</sup>Center for Excellence in Regional Atmospheric Environment, Institute of Urban Environment, Chinese Academy of Sciences, Xiamen, China, <sup>7</sup>Department of Earth and Planetary Sciences, Weizmann Institute of Science, Rehovot, Israel

**Abstract** Atmospheric photooxidation of isoprene forms isoprene epoxydiols (IEPOX) and hydroxymethyl-methyl- $\alpha$ -lactone (HMML) via hydroperoxyl radical (HO<sub>2</sub>) channel and NO/NO<sub>2</sub> channel, respectively. Reactive uptake of these epoxides onto particles produces isoprene secondary organic aerosols (iSOA). Currently, there is little information regarding these two epoxides during iSOA formation in polluted regions. In this study, iSOA tracers from IEPOX and HMML were measured from summer to fall in the heavily polluted Pearl River Delta (PRD) region. The total concentration of the iSOA tracers ranged from 5.77 to 466 ng m<sup>-3</sup>. Isoprene SOA tracers correlated well with sulfate ( $p < 0.01$ ), indicating that the abundant sulfate in the PRD plays an important role in iSOA formation. A kinetic model of IEPOX loss showed that 58% of IEPOX could undergo ring-opening reactions under the polluted PRD conditions in summer. This leads to high levels of IEPOX-derived SOA tracers in the PRD. High temperature in the PRD (>22 °C) suppresses the production of HMML, likely as a result of fast decomposition of HMML's precursor under high temperatures. Thus, the HMML-derived tracers had lower levels than the IEPOX-derived SOA tracers during the whole campaign. The ratios of the IEPOX-derived tracers to the HMML-derived SOA tracers in summer were ~3 times higher than those in fall. This seasonal trend may be explained by the relative high isoprene/NO<sub>x</sub> ratio, temperature, and fast heterogeneous reaction of IEPOX in summer. Our study shows that in highly polluted regions like PRD, reduction in SO<sub>2</sub> emission can significantly reduce iSOA formation.

### 1. Introduction

As a large fraction of organic aerosol (OA), secondary OA (SOA) influences the global climate and has adverse effects on regional air quality and human health. SOA is produced via the oxidation of anthropogenic and biogenic hydrocarbons with ozone (O<sub>3</sub>), hydroxyl radical (OH), and nitrate radical (NO<sub>3</sub>) and followed by nucleation or mass transfer to preexisting particles (Kroll & Seinfeld, 2008; Seinfeld & Pankow, 2003). On a global scale, isoprene (2-methyl-1,3-butadiene, C<sub>5</sub>H<sub>8</sub>) emissions are estimated to be 500–750 Tg yr<sup>-1</sup> and comprise approximately half of the annual global nonmethane hydrocarbon emissions from all natural and anthropogenic sources (Guenther et al., 2006). Isoprene is highly reactive and readily reacts with atmospheric oxidants to form SOA with a yield of 1–28.6% (Kroll et al., 2005, 2006; Ng et al., 2008; Surratt et al., 2010) depending on reaction conditions. The global SOA production from isoprene is estimated to be 19.2 TgC yr<sup>-1</sup>, accounting for ~70% of the total SOA (Heald et al., 2008). Therefore, isoprene plays a key role in the formation of SOA, although recent field, laboratory, and modeling studies have raised many questions regarding the oxidation products and their roles in the SOA formation mechanisms from isoprene (Carlton et al., 2009; Claeys, Graham, et al., 2004; Paulot, Crounse, Kjaergaard, Kürten, et al., 2009; Surratt et al., 2010; Whalley et al., 2014). Nevertheless, SOA yields measured from these previous chamber experiments may not be a reasonable way to parameterize SOA from the multiphase chemistry of isoprene and its oxidation products. Recent studies by Zhang et al. (2018) and Gaston et al. (2014) show that consideration of an organic shell/inorganic aqueous core of an aerosol may be needed to accurately simulate isoprene SOA (iSOA)

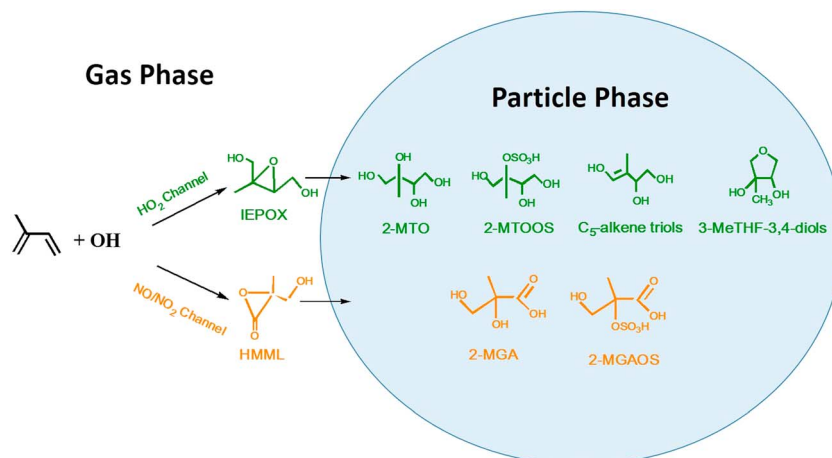


**Figure 1.** The reaction mechanism for the formation of the IEPOX- and HMML-derived tracers from isoprene photooxidation for the HO<sub>2</sub> and NO/NO<sub>2</sub> channels, respectively.

formation. This is starting to become explicitly included in atmospheric models (Pye et al., 2013; Marais et al., 2016; McNeill, 2015).

Isoprene epoxides play key roles in iSOA formation. Through the HO<sub>2</sub> channel, isoprene reacts with the OH and HO<sub>2</sub> radicals to form hydroxy hydroperoxides (ISOPOOH) and then IEPOX in the gas phase (Paulot, Crouse, Kjaergaard, Kürten, et al., 2009). The reactive uptake of IEPOX by acidic particles produces the IEPOX-derived species, including 3-MeTHF-3,4-diols (*cis* and *trans*-3-methyltetrahydrofuran-3,4-diols), 2-methyltetrols (2-MTO: 2-methylthreitol and 2-methylerythritol), C<sub>5</sub>-alkene triols (*cis* and *trans*-2-methyl-1,3,4-trihydroxy-1-butene, 3-methyl-2,3,4-trihydroxy-1-butene), 2-methyltetrol sulfate ester (2-MTOOS), and oligomers (Darer et al., 2011; Lin et al., 2012; Nguyen et al., 2014). Through the NO/NO<sub>2</sub>-channel, intermediates from isoprene oxidation react with nitrogen oxides (NO/NO<sub>2</sub>) to form peroxyacetic nitric anhydride (MPAN). Previous study showed that MPAN decomposition produces methacrylic acid epoxide in the gas phase which can generate SOA via further reactions (Lin, Zhang, et al., 2013). A recent study by Nguyen, Bates, et al. (2015) showed that methacrylic acid epoxide from MPAN is negligible while decomposition of MPAN yields ~75% of hydroxymethyl-methyl- $\alpha$ -lactone (HMML) in the gas phase. The further uptake of HMML by hydrated inorganic particles produces 2-methylglyceric acid (2-MGA), 2-methylglyceric acid sulfate ester (2-MGAOS), and oligomer species (Nguyen, Bates, et al., 2015). In the real atmosphere, the HO<sub>2</sub>-channel and the NO/NO<sub>2</sub>-channel reactions coexist and are competing (Figure 1). Thus, it is essential to understand the relative roles of these two pathways in iSOA production, particularly in the polluted regions that have high emissions of anthropogenic pollutants and isoprene.

The influence of anthropogenic emissions on iSOA formation is complex and undefined. Emissions of NO suppress IEPOX formation due to the inverse dependence of the IEPOX yield on NO concentrations (Paulot, Crouse, Kjaergaard, Kürten, et al., 2009). The GEOS-Chem model predicted that in summer, IEPOX levels over the eastern China (less than 0.1 ppbv) are much lower than those (approximately 0.5 ppbv) over the southeastern United States (SEUS), largely due to the suppression of IEPOX formation from large quantities of anthropogenic emissions (e.g., NO<sub>x</sub>; Paulot, Crouse, Kjaergaard, Kürten, et al., 2009). However, the major IEPOX-derived SOA tracers, 2-MTO, exhibits comparable levels to those observed in the SEUS (as high as hundreds ng m<sup>-3</sup>) at some urban sites in the eastern China during summer (Ding et al., 2008; Ding et al., 2014; Kleindienst et al., 2007; Kleindienst et al., 2010). There should be factors that enhance SOA yield from IEPOX in polluted areas. Acid-catalyzed particle-phase reactions may accelerate iSOA production (Jang et al., 2002; Surratt et al., 2007). High emissions of NO<sub>x</sub> and SO<sub>2</sub> in polluted regions lead to highly acidic particles in the air. Chamber studies have demonstrated that aerosol acidity enhances the SOA yield of IEPOX (Lin et al., 2012; Surratt et al., 2010). Laboratory experiments have also reported a significant enhancement in the rates of IEPOX ring-opening reactions in acidic solutions (Eddingsaas et al., 2010; Minerath et al., 2009). Moreover, recently, aerosol flow tube studies have demonstrated that acid-catalyzed reactive uptake of IEPOX is competitive with other atmospheric loss processes (e.g., dry deposition of IEPOX and gas-phase

reactions with OH radicals; Gaston et al., 2014; Riedel et al., 2015; Zhang et al., 2018). However, in the real atmosphere, the influence of aerosol acidity on IEPOX-derived SOA formation remains unclear. In the air of the highly polluted Pearl River Delta (PRD) region, South China, the slope of the correlation between 2-MTO and aerosol acidity (Ding et al., 2011) was 2 orders of magnitude lower than that observed in a chamber study (Surratt et al., 2007). At a forested site in California, 2-MTOOS exhibited no correlation with aerosol acidity (Worton et al., 2013). In the SEUS, observational studies that investigated the roles of aerosol acidity and sulfate loading at iSOA production found that IEPOX-derived SOA showed a weak correlation with aerosol acidity but exhibited strong correlation with aerosol sulfate (Budisulistiorini et al., 2013, 2015; Lin, Knipping, et al., 2013; Xu et al., 2015, 2016). More recently, modeling and observational studies demonstrated that aerosols in the SEUS are acidic enough to form IEPOX-derived SOA and isoprene oxidation products selectively uptake only on sulfate-containing particles (Budisulistiorini et al., 2017; Liu et al., 2017). More field studies in polluted regions are needed to provide insights into the influence of anthropogenic emissions on iSOA formation.

Increasing  $\text{NO}_x$  levels shift the isoprene oxidation from the  $\text{HO}_2$ -channel to the  $\text{NO}/\text{NO}_2$ -channel (Surratt et al., 2010). Thus, high anthropogenic emissions in urban areas would favor the production of HMML and its SOA. At three urban sites in California, the major HMML-derived SOA tracer, 2-MGA, was dominant over 2-MTO, due to the dominance of the  $\text{NO}/\text{NO}_2$ -channel in iSOA formation (Lewandowski et al., 2013). In the North Pacific Ocean and the Arctic, the majority of 2-MGA was observed (Ding et al., 2013; Fu et al., 2009; Fu et al., 2011), perhaps due to the high  $\text{NO}_x$  emission during the forest fires in the adjacent continent (Ding et al., 2013). However, the prevalence of 2-MGA over 2-MTO was never observed in the highly polluted PRD (Ding et al., 2011; Ding et al., 2012). Additionally, 2-MGAOS was almost undetectable in the PRD during summer and fall in 2010 (He et al., 2014). Thus, we question why HMML-derived SOA products are not abundant in the heavily polluted PRD.

The PRD is located in the subtropics and has an annual average temperature of 25 °C and an annual relative humidity of 70% (Wang et al., 2011). The vegetation in the PRD includes evergreens; thus, biogenic emissions are high throughout the year (Wang et al., 2011). This region has experienced remarkable urbanization and industrialization during the past three decades and is one of the most developed regions in China. With the rapid economic growth, large amounts of anthropogenic pollutants (e.g.,  $\text{NO}_x$  and  $\text{SO}_2$ ) are emitted into the air (Chan & Yao, 2008). High concentrations of sulfate and nitrate make the particles very acidic in the PRD, and the aerosol pH varied from  $-1.0$  to  $0.8$  from 2007 to 2012 (Fu et al., 2015). The elevated surface ozone concentration from 1997 to 2010 indicates that the oxidation capacity of the air has increased in the PRD (Lee et al., 2014). All of these factors make the PRD an ideal place to study biogenic SOA formation under the influence of human activities. In this study, iSOA tracers from the IEPOX and the HMML pathways were analyzed to investigate the role of the two key epoxides in the iSOA formation in this highly polluted region.

## 2. Experimental Section

### 2.1. Field Sampling

Field sampling was conducted at a regional background site, Wanqingsha (WQS, 22°42'N, 113°32'E, Figure S1 in the supporting information), in the PRD. Details of the sampling site and the field campaigns have been described elsewhere (Ding et al., 2012). A high volume sampler (Tisch Environmental Inc., Ohio) was set up on the rooftop of a seven-floor building in the campus of a middle school, to collect fine particles ( $\text{PM}_{2.5}$ ) onto  $8 \times 10$  inch prebaked (500°C for 24 hr) quartz filters at a flow rate of  $1.1 \text{ m}^3 \text{ min}^{-1}$ . The filters were covered with aluminum foil and stored in zipped antistatic bags containing silica gel at 4°C before and  $-20^\circ\text{C}$  after collection. A previous study revealed that isoprene emission in the PRD exhibited less variation from June to September and significantly declined in November and December (Figure S2; Zheng et al., 2010). Our previous study on the SOA tracers has found that the iSOA contributed 18% of the estimated SOC in the PRD, and the contribution could reach the highest of 45% in summer (Ding et al., 2012). Thus, 24-hr sampling was conducted during summer (28 August to 21 September) and fall (10 November to 9 December), in 2008. A total of 52 field samples were collected with four field blanks. Chemical composition analyses for isoprene-derived SOA tracers and inorganic ions were performed within 3 months after the campaign. 2-MTOOS and 2-MGAOS analysis were

performed later in the year 2011. Due to the low storage temperature and dry condition of the filters, the storage time could have limited influence in the organosulfates analysis.

## 2.2. Chemical Analysis

Seven iSOA tracers were analyzed using a gas chromatography/mass spectrometer detector (GC-MSD), including 3-MeTHF-3,4-diols, 2-MTO, 2-MGA, and C<sub>5</sub>-alkene triols. The detailed description of the chemical analysis has been provided previously (Ding et al., 2011; Ding et al., 2012). Briefly, the filters were extracted by sonication with mixed solvents. Prior to the solvent extraction, levoglucosan-<sup>13</sup>C<sub>6</sub> was spiked onto the samples as the internal standard. The extracts of each sample were combined, filtered, and concentrated. After silylation, the derivatives were analyzed by an Agilent 5975 GC-MSD in the scan mode using a 30-m HP-5 MS capillary column. The GC temperature was initiated at 65°C (held for 2 min), increased to 290°C in 45 min, and then kept constant for 20 min. Due to the lack of standards, all of these iSOA tracers were quantified using erythritol (Claeys, Graham, et al., 2004; Ding et al., 2012; Ding et al., 2008; Lin, Knipping, et al., 2013). The detection limit and recovery of erythritol were 0.05 ng m<sup>-3</sup> and 80 ± 9%, respectively. Using the empirical approach developed by Stone et al. (2012), the uncertainties from surrogate quantification (*E<sub>Q</sub>*) were 35%, 15%, 20%, and 85% for 3-MeTHF-3,4-diols, 2-MTO, 2-MGA, and C<sub>5</sub>-alkene triols, respectively (Text S1 and Table S1 in the supporting information). Total ion chromatograms and extracted ion chromatograms for the detected compounds are shown in Figure S2. In addition, it is worth noting that recent studies have argued that part of detected isoprene-derived SOA tracers like 2-MTO, 3-MeTHF-3,4-diols, and C<sub>5</sub>-alkene triols are derived from thermal decomposition products of accretion products (like oligomers of IEPOX) or other low volatility organics (Hu et al., 2015; Lopez-Hilfiker et al., 2016). To address this issue, we analyze the composition of C<sub>5</sub>-alkene triol isomers. If thermal decomposition during GC-MSD analysis is a major source of the detected C<sub>5</sub>-alkene triols, we expect the composition (ratios of the isomers) of the C<sub>5</sub>-alkene triols to be similar in different samples. In fact, we found that the relative abundances of the three C<sub>5</sub>-alkene triol isomers vary from sample to sample (Figure S3). This suggests that the GC-MSD measured C<sub>5</sub>-alkene triols are not mainly derived from the thermal decomposition and that they do reflect the formation processes/pathways under different conditions in the atmosphere.

The organosulfates from IEPOX and HMML were analyzed using liquid chromatography/mass spectrometer, including 2-MTOOS and 2-MGAOS. The detailed description of the chemical analysis is elsewhere (He et al., 2014). Briefly, a punch ( $\Phi = 47$  mm) of each filter was taken and extracted twice via sonication with methanol. Before extraction, ketopinic acid was spiked onto the filters as the internal standard. The extracts were combined, concentrated, centrifuged, and syringe filtered. The remaining liquid was then evaporated to near dryness and redissolved in 500  $\mu$ L of a 1:1 (vol/vol) solvent mixture of 0.1% acetic acid in water and 0.1% acetic acid in methanol. The sample extracts were analyzed by an Agilent 6410 Triple Quadrupole liquid chromatography/mass spectrometer equipped with an electrospray ionization (ESI) source operated in negative ion mode. A Waters Atlantic T3 column was employed to isolate the compounds. The eluents were water with 0.1% acetic acid (eluent A) and methanol (eluent B) with a total flow rate of 0.2 mL min<sup>-1</sup>. The gradient of the mobile phase was set as follows: started with 3% B and kept constant for 5 min, increased to 90% B in 25 min, kept constant for 10 min and then increased to 95% B in 2 min, kept constant for 6 min, finally decreased to 3% B in 5 min, and finally held for constant for 12 min until the pump pressure balanced. The ESI tandem MS was operated under a nebulizer pressure 0.8 bar and a dry gas flow of 10 L min<sup>-1</sup>. Due to the lack of standards, camphor sulfonic acid was used to quantify the organosulfates (He et al., 2014; Kristensen & Glasius, 2011; Worton et al., 2011). The detection limit and recovery were 0.02 ng m<sup>-3</sup> and 94 ± 4%, respectively. Comparison study on synthesized standards reveals that camphor sulfonic acid is an appropriate quantification surrogate when using [M-H]<sup>-</sup> as quantification ion (Wang et al., 2017). A solution of camphor sulfonic acid was used to optimize the ionization and fragmentation parameters to gain a high intensity of the [M-H]<sup>-</sup> for quantification. The final employed ionization voltage was 4 kV, and the fragmentor was 120 V. The total ion chromatograms and extracted ion chromatograms for the detected compounds are shown in Figure S2. As we can see from Figure S2, 2-MTOOS and 2-MGAOS coelute with sulfate. Due to different sulfate levels in the samples, the ESI conditions for these two compounds might vary from sample to sample, which could cause the quantification off for these tracers. To address this issue, ammonium sulfate solution spiked filters (cut from one filter sample in this campaign) with different equivalent sulfate concentrations (24.6, 33.5, 39.5, 42.5, and 48.5  $\mu$ g m<sup>-3</sup>) were analyzed. The quantified 2-MTOOS and 2-MGAOS

concentrations are independent of the sulfate concentration, indicating a limited influence of sulfate in 2-MTOOS and 2-MGAOS quantification. The use of camphor sulfonic acid as surrogate standards adds uncertainty to the absolute concentrations of 2-MTOOS and 2-MGAOS since ESI response factors may be different for different compounds (Worton et al., 2011). Nevertheless, these data in this study can still provide important information on time-dependent variation in levels.

A punch (1.5 × 1.0 cm) of each filter was taken to measure organic carbon (OC) and elemental carbon using the thermo-optical transmittance method (NIOSH, 1999) with an OC/EC Analyzer (Sunset Laboratory Inc.). An additional punch ( $\Phi = 25.4$  mm) was taken and ultrasonically extracted with 18-MO $\Omega$ m milli-Q water to analyze sulfate (SO<sub>4</sub><sup>2-</sup>), nitrate (NO<sub>3</sub><sup>-</sup>), and ammonium (NH<sub>4</sub><sup>+</sup>) using an ion chromatography (Metrohm 883, Switzerland; Fu et al., 2014).

### 2.3. Calculation of Aerosol Acidity

The thermodynamics model ISORROPIA-II (Nenes et al., 1998) was used to predict aerosol pH. Due to the lack of gas phase chemicals (e.g., NH<sub>3</sub>, HNO<sub>3</sub>, and HCl) data, we calculated the aerosol pH by performing iterations using the forward model. That is, only aerosol phase data input was used for the first run of the forward model (Guo et al., 2015; Hennigan et al., 2015). Then added the output gas-phase concentrations from the first run to the initial aerosol phase chemical concentrations to derive total (gas and aerosol) concentration which serves as input for the second run. Subsequent iterations could lead to convergence of gas-phase concentrations. Finally, with the input of total (convergent gas + aerosol) concentrations of aerosol precursors in the air, temperature, and relative humidity, we calculated the aerosol pH and liquid water content (LWC). For example, for the sample collected on 3 September (Figures S4a–S4c), the total ammonia concentration (gas phase NH<sub>3</sub> and aerosol phase NH<sub>4</sub><sup>+</sup>), LWC, and aerosol pH converged after 72 iterations. Additionally, the model predicted aerosol phase NH<sub>4</sub><sup>+</sup> and SO<sub>4</sub><sup>2-</sup> agree well with the measured results (Figures S4d and S4e), indicating that the iteration method provides reliable pH estimation. Previous studies have demonstrated that the inclusion of organic species in the calculation of aerosol LWC changes predicted values by less than 20% (Aggarwal et al., 2007; Liu et al., 2012; Speer et al., 2003). Moreover, the concentrations of water-soluble organic acids in Chinese megacities constituted only about 1–4% of the total ions (Huang et al., 2005; Yao et al., 2004), indicating a negligible impact of organics on the LWC and the acidity estimated by the ISORROPIA-II (Aggarwal et al., 2007; Liu et al., 2012; Speer et al., 2003). Thus, organics are ignored in LWC and pH estimation.

## 3. Results and Discussion

The sum of all the iSOA tracers ranged from 5.77 to 466 ng m<sup>-3</sup> with an average of 70.4 ± 111 ng m<sup>-3</sup>. Among these tracers, 2-MTOs were the major compounds, with the average level of 48.0 ± 79.7 ng m<sup>-3</sup>, followed by C<sub>5</sub>-alkene triols (13.9 ± 25.3 ng m<sup>-3</sup>), 2-MGA (6.00 ± 5.03 ng m<sup>-3</sup>), 2-MGAOS (1.27 ± 1.15 ng m<sup>-3</sup>), and 2-MTOOS (1.08 ± 2.42 ng m<sup>-3</sup>). 3-MeTHF-3,4-diols were found only in trace amounts (0.31 ± 0.42 ng m<sup>-3</sup>). All of the iSOA tracers exhibited higher levels in summer than in fall (Figure S5), probably due to greater emissions of isoprene under the high temperature and intense light during summer in the PRD (Ding et al., 2012). Table 1 summarizes the iSOA tracers in the air of PRD.

### 3.1. Tracers Formed From the IEPOX Pathway

The total IEPOX-derived tracers had an average concentration of 121 ± 144 ng m<sup>-3</sup> in summer and 20.8 ± 17.0 ng m<sup>-3</sup> in fall. 3-MeTHF-3,4-diols that are produced by the acid-catalyzed intermolecular rearrangement of IEPOX in the acidic particles (Lin et al., 2012) were first reported in the PRD. Their average levels were 0.44 (nd – 2.17) ng m<sup>-3</sup> in summer and 0.19 (nd – 0.64) ng m<sup>-3</sup> in fall. The levels of 3-MeTHF-3,4-diols in the PRD were approximately 1 order of magnitude lower than those in the SEUS (Figure 2a; Chan et al., 2010; Lin, Knipping, et al., 2013; Lin et al., 2012). A previous modeling study predicted that IEPOX concentrations in the PRD during summer were much lower than those in the SEUS (Paulot, Crouse, Kjaergaard, Kürten, et al., 2009), likely due to the suppression of IEPOX production under high NO<sub>x</sub> levels in the PRD (He et al., 2014). The hourly and daily NO<sub>2</sub> levels at WQS, which were monitored by the PRD regional air quality monitoring network (<http://www.gdep.gov.cn/hjjce/kqjc/201204/P020120423559911259055.pdf>), were as high as 144 and 82 ppbv, respectively, in 2008 (Figure S6). Thus, 3-MeTHF-3,4-diols were found only in trace amounts in the PRD. The two isomers, *cis*- and *trans*-3-MeTHF-3,4-diol exhibited significant correlations with



**Table 1**  
Summary of Tracers in the Air of PRD

	Summer				Fall			
	Mean	Med	Min	Max	Mean	Med	Min	Max
SO <sub>4</sub> <sup>2-</sup> (μg m <sup>-3</sup> )	23.0	21.7	8.40	46.8	15.9	15.1	7.97	29.8
NO <sub>3</sub> <sup>-</sup> (μg m <sup>-3</sup> )	5.26	4.22	1.28	12.6	8.88	7.83	2.73	22.6
NH <sub>4</sub> <sup>+</sup> (μg m <sup>-3</sup> )	4.92	4.62	2.13	10.7	5.26	4.96	0.62	11.0
Temperature(°C)	29.0	29.2	25.8	31.3	22.6	22.1	17.6	27.6
RH (%)	66	65	54	81	47	47	23	73
LWC	24.5	24.0	10.9	44.3	11.8	11.1	1.17	25.0
pH	0.51	-0.02	-0.37	2.36	2.76	3.16	-0.44	4.73
IEPOX-derived SOA tracers (ng m <sup>-3</sup> )								
2-MeTHF-3,4-diols	0.44	0.26	nd	2.17	0.19	0.13	nd	0.64
C <sub>5</sub> -alkene triols	26.9	8.13	0.48	113	4.29	3.08	0.40	15.1
2-Methyltetrols (2-MTO)	91.5	49.2	4.97	319	16.0	10.3	2.34	58.3
2-Methyltetrol sulfate ester (2-MTOOS)	2.20	0.53	nd	12.4	0.30	0.31	nd	0.77
Sum of IEPOX-derived tracers	121	58.2	5.89	435	20.8	13.7	3.12	72.2
HMML-derived SOA tracers (ng m <sup>-3</sup> )								
2-Methylglyceric acid (2-MGA)	7.71	6.45	0.86	25.9	4.75	4.03	1.40	14.7
2-MGA sulfate ester (2-MGAOS)	1.40	0.92	nd	6.55	1.18	1.10	nd	2.86
Sum of HMML-derived tracers	9.05	7.55	0.95	30.6	5.93	5.36	2.47	16.3

Note. "nd" means below the detection limit; "Med" represents "median."

each other in both seasons ( $p < 0.01$ , Figure 2b). The slopes were comparable in summer (0.57) and fall (0.59), indicating that the relative formation rates of these two isomers were stable in summer and fall. The direct ring-opening reactions of IEPOX on acidic particles can form 2-MTO and 2-MTOOS by the nucleophilic addition of water and sulfate, respectively (Lin et al., 2012; Lin, Zhang, et al., 2013; Surratt et al., 2010).

Because they share the same precursors, 2-MTO and 2-MTOOS correlated well with each other (Figure 3a). The ratio of 2-MTOOS to 2-MTO (2-MTOOS/2-MTO) was  $0.028 \pm 0.029$  at WQS, indicating that the nucleophilic addition of water to the IEPOX ring was much more effective than that of sulfate at WQS.

All of the detected IEPOX-derived iSOA tracers exhibited positive correlation with sulfate (Table S2,  $p < 0.01$ ,  $R^2$  0.47–0.60). This suggests that sulfate has an important influence on IEPOX SOA formation at WQS, which is consistent with the observations in the SEUS (Budisulistiorini et al., 2015; Liu et al., 2017; Xu et al., 2015). Xu et al. (2015) pointed out that sulfate can control IEPOX-SOA formation by the concerted nucleophilic addition to the IEPOX ring and/or via the salting-in effect that influences the solubility of IEPOX. Recent studies (Budisulistiorini et al., 2017; Riedel et al., 2016; Xu et al., 2016; Zhang et al., 2018) have demonstrated that the pseudo first-order heterogeneous reaction rate constant for IEPOX reactive uptake linearly correlates with particle surface area. Higher sulfate in the aerosol increases the number of active surface sites for reactive uptake process. Since the sulfate levels were much higher in the PRD than the SE US. ( $23.0$  versus  $1.7 \mu\text{g m}^{-3}$ ), such a direct influence of sulfate on IEPOX SOA formation may be more pronounced in the PRD and promotes iSOA formation.

Due to the suppression of IEPOX production by high NO<sub>x</sub> levels, the concentrations of all the tracers formed through IEPOX pathway were thought to be lower in the PRD compared with the SEUS. Our observations demonstrated that the rearrangement products of IEPOX, 3-MeTHF-3,4-diols were indeed in low concentrations in the PRD (Figure 2a). However, the concentrations of the ring-opening products, 2-MTO (Figure S7), were comparable

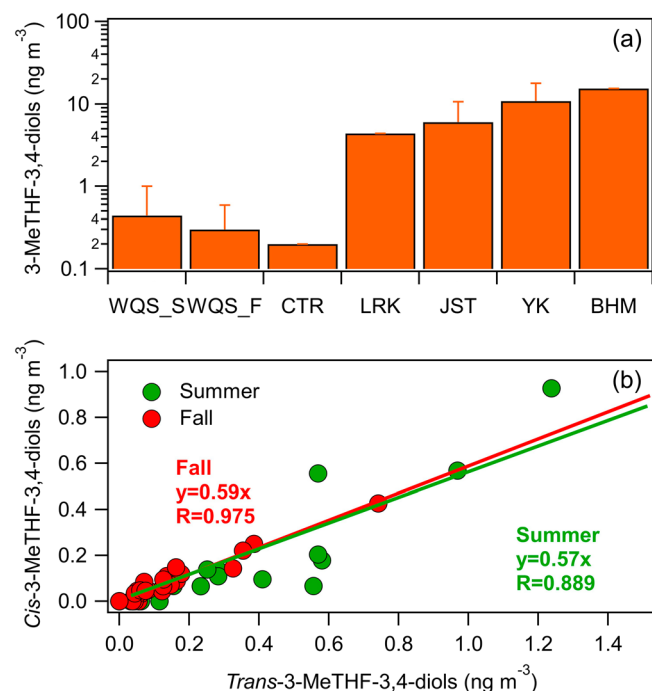


**Figure 2.** (a) 3-MeTHF-3,4-diol concentrations at WQS (Wanqingsha site), JST (Jefferson Street site in Atlanta, GA), YK (a rural site in Yorkville, GA; Chan et al., 2010); BHM (a urban site in Birmingham, AL), CTR (a rural site Centreville, AL), and LRK (a rural site in Look Rock, TN). (b) Correlations between 3-MeTHF-3,4-diol isomers in summer and fall at WQS.

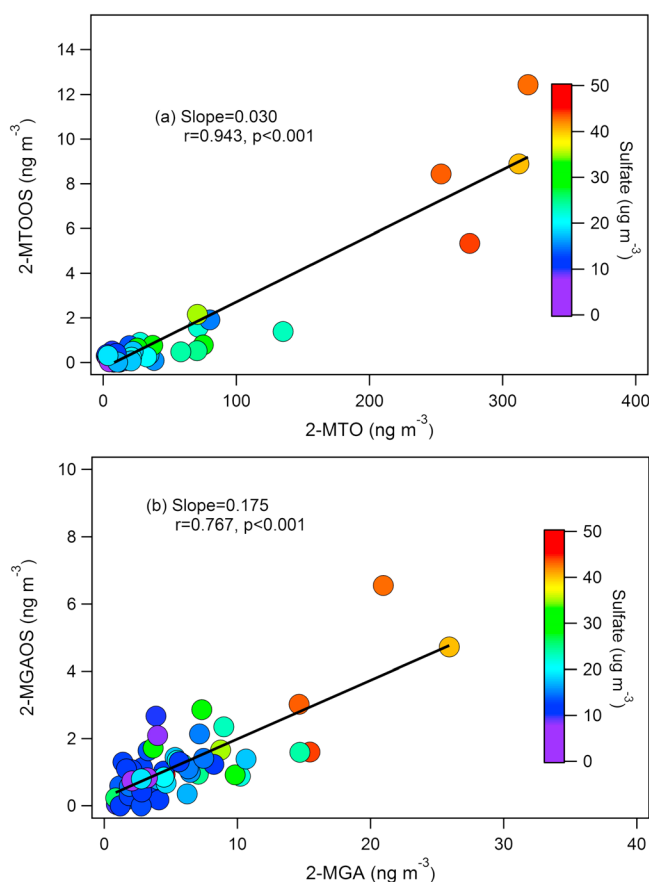


**Figure 3.** Correlations between (a) 2-MTOOS and 2-MTO and (b) 2-MGAOS and 2-MGA. The correlations between sulfate and tracers are all significant ( $p < 0.001$ ).

between the PRD and the SEUS (Budisulistiorini et al., 2015; Chan et al., 2010; Ding et al., 2008, 2014; Kleindienst et al., 2007, 2010; Lin, Knipping, et al., 2013; Rattanavaraha et al., 2016) and less polluted regions (Claeys, Wang, et al., 2004; El Haddad et al., 2011; Ion et al., 2005; Kourtchev et al., 2005; Lewandowski et al., 2013). Therefore, other factors must accelerate the ring-opening reactions of IEPOX in the PRD.

Gas phase IEPOX is removed via three main processes: (1) OH oxidation in the gas phase (Bates et al., 2014), (2) ring-opening reactions in the particle-phase (Eddingsaas et al., 2010; Nguyen et al., 2014; Surratt et al., 2006), and (3) dry deposition. Using the kinetic Kintecus model (Benter et al., 1994), Eddingsaas et al. (2010) evaluated the influence of aerosol pH and LWC on the relative contributions of the three pathways that lead to the IEPOX termination. Worton et al. (2013) applied the Kintecus model to estimate the relative contributions of the three pathways for IEPOX in Sierra Nevada Mountains. In this study, we employed the same model to estimate the relative contribution of the three pathways to the IEPOX termination in the air of the PRD. As discussed above, the particle surface area which relates to the aerosol sulfate played an important role in IEPOX's fate. Since the Kintecus model we used does not include the particle surface area, the model predicted results only represent the upper limit.

Two measurements exist for the gas-phase IEPOX oxidation rate constant ( $k$ ) at 298 K:  $1.52 \pm 0.07 \times 10^{-11} \text{ cm}^3 \text{ molecule}^{-1} \text{ s}^{-1}$  (Bates et al., 2014) and  $3.60 \pm 0.76 \times 10^{-11} \text{ cm}^3 \text{ molecule}^{-1} \text{ s}^{-1}$  (Jacobs et al., 2013). Paulot, Crouse, Kjaergaard, Kürten, et al. (2009) estimated the relationship between temperature ( $T$ ) and the upper bound of the rate constant as  $k(T) = 5.78 \times 10^{-11} \exp(-400/T)$ . At  $T = 298 \text{ K}$ , the rate constant is calculated to be  $1.51 \times 10^{-11} \text{ cm}^3 \text{ molecule}^{-1} \text{ s}^{-1}$ , which is consistent with the value reported by Bates et al. (2014). Thus, the rate constant of  $1.52 \times 10^{-11} \text{ cm}^3 \text{ molecule}^{-1} \text{ s}^{-1}$  was used in our calculation. Several studies were performed to investigate the OH radical concentration in China. Lu et al. (2013) detected that daily concentration maximum of OH radical was in the range of  $(4\text{--}17) \times 10^6 \text{ molecules cm}^{-3}$  in Beijing. Nan et al. (2017) observed that the daytime OH radical concentration in Shanghai under steady state was averaged at  $1.0 \times 10^7 \text{ molecules cm}^{-3}$ . The average OH level in the PRD during daytime in summer was about  $1.0 \times 10^7 \text{ molecules cm}^{-3}$  (Hofzumahaus et al., 2009). Thus, the gas phase IEPOX oxidation rate ( $k_{\text{ox-IEPOX}}$ ) at 298 K could be  $1.52 \times 10^{-4} \text{ s}^{-1}$  at daytime with OH radical concentration of  $1.0 \times 10^7 \text{ molecules cm}^{-3}$ .

Particle-phase ring-opening processes involve gas to particle partitioning followed by aqueous phase ring-opening reactions. The subcooled vapor pressure of IEPOX is estimated to be  $4.9 \times 10^{-6} \text{ atm}$ , suggesting that the gas partitioning into the organic matter was negligible for IEPOX because of its high volatility (Worton et al., 2013). The partitioning of IEPOX into the aqueous phase is governed by the Henry law constant ( $k_{\text{H}}^{\text{CP}}$ ). Chan et al. (2010) estimated the  $k_{\text{H}}^{\text{CP}}$  of IEPOX to be in the range of  $1.9 \times 10^6$  to  $9.6 \times 10^8 \text{ M atm}^{-1}$ . Estimated  $k_{\text{H}}^{\text{CP}}$  from other studies (Eddingsaas et al., 2010; Gaston et al., 2014; Nguyen et al., 2014; Nguyen, Crouse, et al., 2015; Pye et al., 2013) are all within the range. It should be noted that the atmospheric fate of IEPOX is sensitive to the  $k_{\text{H}}^{\text{CP}}$  values used in the model. As Figure S8 shows, the contribution of the particle phase ring-opening reactions to the total loss of IEPOX ( $F_{\text{top-IEPOX}}$ ) exhibited a huge difference by 2 orders of magnitude between the upper and lower limits under the typical summer conditions in the PRD ( $\text{LWC} = 24.5 \mu\text{g m}^{-3}$  and  $\text{pH} = 0.51$ ). The  $k_{\text{H}}^{\text{CP}}$  was estimated to be  $1.3 \times 10^8 \text{ M atm}^{-1}$  by Eddingsaas et al. (2010). Gaston et al. (2014) found that the predicted IEPOX reaction probability agreed well with  $k_{\text{H}}^{\text{CP}}$  of  $1.7 \times 10^8 \text{ M atm}^{-1}$ . Thus,  $1.3 \times 10^8 \text{ M atm}^{-1}$  was used in this study. The ring-opening rate constants were determined to be  $0.036 \text{ M}^{-1} \text{ s}^{-1}$  for  $\beta$ -IEPOX, and up to  $0.0079 \text{ M}^{-1} \text{ s}^{-1}$  for  $\delta$ -IEPOX (Cole-Filipiak et al., 2010). Because  $\beta$ -IEPOX accounts for  $\sim 70\%$  of total IEPOX in the air (Paulot, Crouse, Kjaergaard, Kroll, et al., 2009), the experimental value for  $\beta$ -IEPOX ( $0.036 \text{ M}^{-1} \text{ s}^{-1}$ ) was used in our simulation.

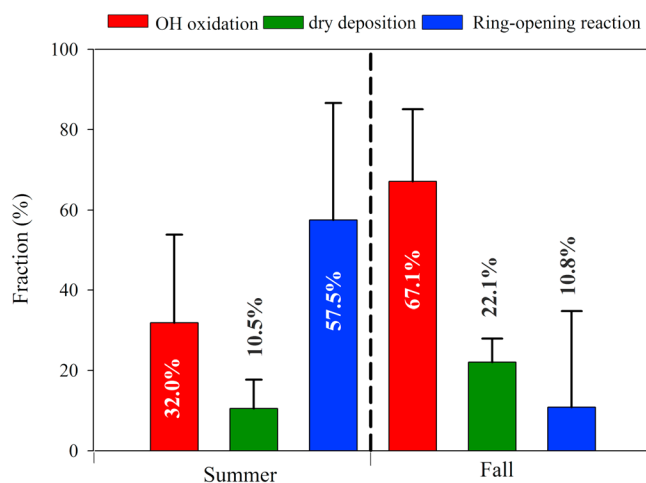


**Figure 4.** Relative contributions of OH oxidation ( $F_{\text{ox}}$ ), dry deposition ( $F_{\text{dd}}$ ), and particle-phase ring-opening reactions ( $F_{\text{rop}}$ ) for IEPOX loss at WQS.

The dry deposition rate ( $k_{\text{dd}}$ ) is determined by the deposition velocity and the boundary layer height. Nguyen, Crouse, et al. (2015) measured the deposition velocity of IEPOX of  $2.5 \text{ cm s}^{-1}$ . The boundary height of the PRD was  $\sim 500 \text{ m}$  in summer (Fan et al., 2011), suggesting  $k_{\text{dd}} = 5 \times 10^{-5} \text{ s}^{-1}$  in the PRD.

Table S3 summarizes all the parameters for the IEPOX termination in this study. The kinetic simulation was conducted for 72 hr to ensure the complete loss of IEPOX. Figure S9 presents the influence of the aerosol pH and LWC on  $F_{\text{rop-IEPOX}}$ . The  $F_{\text{rop-IEPOX}}$  increases with a decreasing pH and an elevated LWC. During our campaign, the aerosol pH was estimated to be 0.51 in summer and 2.76 in the winter, and the LWC was on average of 24.5 and  $11.8 \mu\text{g m}^{-3}$ , respectively (Table 1). Thus, the  $F_{\text{rop-IEPOX}}$  in the PRD were 57.5% and 10.9% in summer and fall, respectively (Figure 4), indicating that ring-opening reactions are significant processes for iSOA formation in the PRD. Using the measured uptake kinetics, Gaston et al. (2014) found that the predicted lifetime of IEPOX is only a few hours when aerosol pH was below zero. But IEPOX reactive uptake would not be competitive when the pH shifts to  $>2$ . This is consistent with our projection that the

$F_{\text{rop-IEPOX}}$  would be lower than 10% at pH above 2 (Figure S9). The  $F_{\text{rop-IEPOX}}$  values in the PRD are substantially higher than those (0.02%) estimated in Sierra Nevada Mountains (Worton et al., 2013). Guo et al. (2015) reported the median values of aerosol pH and LWC for SEUS during summer. The averaged values for the pH and LWC were 1.1 and  $5.22 \mu\text{g m}^{-3}$ , respectively. Under OH radical level of  $2 \times 10^6 \text{ molecules cm}^{-3}$  in the SEUS (Guo et al., 2015; Xu et al., 2015),  $F_{\text{rop-IEPOX}}$  can be estimated to be 30% in summer, assuming that the other parameters for the SEUS are similar to those in the PRD. Compared with the SEUS, the PRD has higher  $F_{\text{rop-IEPOX}}$ , implying that IEPOX elimination through particle-phase ring-opening reactions plays a more significant role in iSOA formation in the PRD than in the SEUS. As discussed earlier, the aerosol sulfate concentration in the PRD is much higher than that in the SEUS, which implies that the heterogeneous reactive uptake process in the PRD is much faster than in the SEUS. Here we conclude that the enhanced heterogeneous reactions by high sulfate concentration, aerosol acidity, and LWC determine the IEPOX ring-opening products levels in the heavily polluted PRD.

### 3.2. Tracers Formed From HMML Pathway

The direct ring-opening reactions of HMML on hydrated particles can form 2-MGA and 2-MGAOS by nucleophilic addition of water and sulfate, respectively (Lin, Zhang, et al., 2013; Surratt et al., 2010). Thus, 2-MGA and 2-MGAOS correlated well with each other (Figure 3b). Both 2-MGA and 2-MGAOS at WQS exhibited positive correlations with sulfate (Figure 3b,  $p < 0.001$ ,  $R^2$  0.31–0.49), suggesting that sulfate promotes HMML SOA formation. Similar to IEPOX, sulfate also increases the solubility of HMML by salting-in effect, enhances the ring-opening reactions by providing abundant nucleophilic reagents (Xu et al., 2015), and promotes the reactive uptake process by providing more surface area (Budisulistiorini et al., 2017; Riedel et al., 2016; Xu et al., 2016; Zhang et al., 2018). This direct influence of sulfate on HMML SOA formation is important in the PRD due to high sulfate levels.

Due to the high  $\text{NO}_x$  levels (Figure S2), the levels of HMML-derived tracers were thought to be high in the heavily polluted PRD. However, the HMML-derived tracers were more than 1 order of magnitude lower than the IEPOX-derived tracers in summer ( $121 \text{ ng m}^{-3}$  versus  $9.05 \text{ ng m}^{-3}$  on average). Even in fall, when the  $\text{NO}_x$  levels increased and the isoprene emission decreased (Figure S2), the HMML-derived tracers were still lower by a factor of 3.5 ( $20.8 \text{ ng m}^{-3}$  versus  $5.93 \text{ ng m}^{-3}$  on average). This suggests that other factors in the PRD control HMML SOA formation rather than  $\text{NO}_x$  levels.

As observed by Worton et al. (2013), temperature is vital to the fate of MPAN, which is the precursor of HMML. When the temperature exceeds  $20 \text{ }^\circ\text{C}$ , thermal decomposition of MPAN to form peroxy-methacryoyl radical is very fast compared to its reformation. At WQS, the temperature was  $29.0 \text{ }^\circ\text{C}$  in summer and  $22.6 \text{ }^\circ\text{C}$  in fall (Table 1). Based on the rate constants provided by the MCM3.2 (<http://mcm.leeds.ac.uk/MCMv3.2/roots.htm>) and the average temperature obtained in this study, the





fall than those in summer. As a result, the ring-opening reactions of IEPOX played a dominant role in summer (58%) while only had a minor role (11%) in fall in IEPOX removal. Instead, less acidified particles in fall favor the HMML-derived SOA tracers (e.g., 2-MGA) partitioning into the particles (Nguyen, Bates, et al., 2015). All of these lead to higher I/H ratios in summer.

#### 4. Conclusions and Atmospheric Implications

In this study, tracers for isoprene-derived SOA were analyzed in the samples collected during summer and fall at a regional background site in the heavily polluted PRD region. The parameters controlling iSOA formation, especially the HO/HO<sub>2</sub> channel and NO/NO<sub>2</sub> channel, were considered. We found that 3-MeTHF-3,4-diols were only in trace amounts in the PRD. Interestingly, the levels of IEPOX ring-opening products (C<sub>5</sub>-alkene triols and 2-methyltetrols) in the PRD were comparable to those in the SEUS, probably due to the enhanced reactive uptake process due to high levels of aerosol sulfate and the significant IEPOX removal by ring-opening processes. The HMML-derived tracers were present at lower concentrations as compared with IEPOX-derived tracers, largely due to the high temperature in the PRD that suppresses the production of HMML. This study demonstrates that even in highly polluted PRD, the HO<sub>2</sub> channel for iSOA formation is still the dominant pathway.

Recent studies demonstrated that iSOA can be also formed through nonepoxides pathways. Riva, Budisulistiorini, Zhang, et al. (2016) showed that ozonolysis of isoprene in the presence of acidic aerosol yields 2-MTO and unique organosulfates. Considering the dramatic difference in the reaction rate constants of isoprene oxidation by OH radical ( $9.9 \times 10^{-11} \text{ cm}^3 \text{ molecule}^{-1} \text{ s}^{-1}$ ) and by ozone ( $1.3 \times 10^{-17} \text{ cm}^3 \text{ molecule}^{-1} \text{ s}^{-1}$ ), and high OH radical concentrations in the PRD (Hofzumahaus et al., 2009), isoprene should be mainly oxidized by OH radical instead of by ozone. This limits the production of 2-MTO from isoprene ozonolysis in the PRD. Chamber studies in isoprene photooxidation under the HO<sub>2</sub>-dominated conditions (5–10 times higher than atmospherically relevant concentrations) in the absence of heterogeneous IEPOX chemistry found that the iSOA yields could be as high as 15% (Liu et al., 2016) and proposed that ISOPOOH-derived SOA through non-IEPOX routes might account for the high yields (Riva, Budisulistiorini, Chen, et al., 2016). However, in the real atmosphere, the oxidation of ISOPOOH by OH radical can produce IEPOX at yields greater than 75% (St. Clair et al., 2016). Considering the presence of highly acidified particles in the PRD, the IEPOX pathway should play a major role in iSOA formation compared with the non-IEPOX pathways.

In the PRD, the high aerosol-phase sulfate level plays an important role in iSOA formation. As Figure S10 shows, IEPOX-derived SOA tracers correlated positively with sulfate ( $R^2 > 0.43$ ,  $p < 0.001$ ), with slopes of 8.7 and 2.2 in summer and fall, respectively. HMML-derived SOA tracers also correlated with sulfate with a smaller slope (0.47) in fall than in summer (0.25). Such a sulfate dependence of iSOA tracers indicates that a decrease of  $1 \mu\text{g m}^{-3}$  of the sulfate concentration leads to detected IEPOX/HMML-derived SOA tracers reduction by  $8.7/0.47 \text{ ng m}^{-3}$  in summer and  $2.2/0.25 \text{ ng m}^{-3}$  in the winter. Previous studies observed an association between OC and sulfate based on a statistical analysis of the long-term SEARCH data (Blanchard et al., 2016). The authors suggested that the future decrease in sulfate concentration by  $1 \mu\text{g m}^{-3}$  would reduce OA concentration by 0.2 to  $0.35 \mu\text{g m}^{-3}$  (assuming OA/OC = 1.4). Studies based on ground site and airborne measurements through SEUS have demonstrated that decrease in sulfate concentration by  $1 \mu\text{g m}^{-3}$  would reduce OA concentration by 0.23 to  $0.42 \mu\text{g m}^{-3}$  (Xu et al., 2015; Xu et al., 2016). Considering that the detected iSOA tracers only account for part of the iSOA, the effect of sulfate reduction on iSOA maybe more pronounced and comparable with the finding in the SEUS. By applying the magnitude of sulfate effect on iSOA tracers obtained from this study, reducing aerosol sulfate by 25% could cause IEPOX-derived SOA tracers reduction by ~45% and HMML-derived SOA tracers decrease by ~20% in the PRD. This effect is consistent with previous findings in the United States, that lowering SO<sub>x</sub> emissions by 25–48% would lower IEPOX-derived SOA formation by 35 to 70% (Budisulistiorini et al., 2017; Marais et al., 2016; Pye et al., 2013). This study suggests that reducing SO<sub>2</sub> emissions in the PRD could lower both aerosol phase sulfate and iSOA formation. These results highlight the importance of controlling anthropogenic pollutant emissions (e.g., SO<sub>2</sub>) for reducing particle pollution in polluted regions. However, this estimation may serve as an upper bound because the IEPOX concentration is expected to be higher, considering that ambient NO<sub>x</sub> levels may be substantially lower in the future due to emission regulations (Gu et al., 2013). More recently, Zhang et al.

(2018) found that the reactive uptake coefficient of IEPOX ( $\gamma_{\text{IEPOX}}$ ) can be reduced by half when SOA coatings are present prior to uptake. As OA keeps reducing in the future, the coating effect could be less important and a larger  $\gamma_{\text{IEPOX}}$  will be expected. Thus, the formation of IEPOX-derived SOA could be enhanced then and could potentially alter the role of sulfate in iSOA formation.

#### Acknowledgments

This research was supported by the National Science Foundation of China (NSFC; 41722305/41473099/41530641), the State Key Laboratory of Organic Geochemistry (SKLOGA201603A), and the "Outstanding Young Scientist Project" of Youth Innovation Promotion Association, CAS. All the detected isoprene-derived SOA tracers data can be found in the supporting information.

#### References

- Aggarwal, S. G., Mochida, M., Kitamori, Y., & Kawamura, K. (2007). Chemical closure study on hygroscopic properties of urban aerosol particles in Sapporo, Japan. *Environmental Science & Technology*, 41(20), 6920–6925. <https://doi.org/10.1021/es063092m>
- Bates, K. H., Crounse, J. D., St Clair, J. M., Bennett, N. B., Nguyen, T. B., Seinfeld, J. H., et al. (2014). Gas phase production and loss of isoprene epoxydiols. *Journal of Physical Chemistry A*, 118(7), 1237–1246. <https://doi.org/10.1021/Jp4107958>
- Benter, T., Liesner, M., Schindler, R. N., Skov, H., Hjorth, J., & Restelli, G. (1994). Rempi-MS and FTIR study of NO<sub>2</sub> and oxirane formation in the reactions of unsaturated hydrocarbons with NO<sub>3</sub> radicals. *Journal of Physical Chemistry*, 98(41), 10,492–10,496. <https://doi.org/10.1021/J100092a018>
- Blanchard, C. L., Hidy, G. M., Shaw, S., Baumann, K., & Edgerton, E. S. (2016). Effects of emission reductions on organic aerosol in the southeastern United States. *Atmospheric Chemistry and Physics*, 16(1), 215–238. <https://doi.org/10.5194/acp-16-215-2016>
- Budisulistiorini, S. H., Canagaratna, M. R., Croteau, P. L., Marth, W. J., Baumann, K., Edgerton, E. S., et al. (2013). Real-time continuous characterization of secondary organic aerosol derived from isoprene epoxydiols in downtown Atlanta, Georgia, using the aerodyne aerosol chemical speciation monitor. *Environmental Science & Technology*, 47(11), 5686–5694. <https://doi.org/10.1021/Es400023n>
- Budisulistiorini, S. H., Li, X., Bairai, S. T., Renfro, J., Liu, Y., Liu, Y. J., et al. (2015). Examining the effects of anthropogenic emissions on isoprene-derived secondary organic aerosol formation during the 2013 Southern Oxidant and Aerosol Study (SOAS) at the Look Rock, Tennessee ground site. *Atmospheric Chemistry and Physics*, 15(15), 8871–8888. <https://doi.org/10.5194/acp-15-8871-2015>
- Budisulistiorini, S. H., Nenes, A., Carlton, A. G., Surratt, J. D., McNeill, V. F., & Pye, H. O. T. (2017). Simulating aqueous-phase isoprene-epoxydiol (IEPOX) secondary organic aerosol production during the 2013 Southern Oxidant and Aerosol Study (SOAS). *Environmental Science & Technology*, 51(9), 5026–5034. <https://doi.org/10.1021/acs.est.6b05750>
- Carlton, A. G., Wiedinmyer, C., & Kroll, J. H. (2009). A review of secondary organic aerosol (SOA) formation from isoprene. *Atmospheric Chemistry and Physics*, 9(14), 4987–5005. <https://doi.org/10.5194/acp-9-4987-2009>
- Chan, C. K., & Yao, X. (2008). Air pollution in mega cities in China. *Atmospheric Environment*, 42(1), 1–42. <https://doi.org/10.1016/j.atmosenv.2007.09.003>
- Chan, M. N., Surratt, J. D., Claeys, M., Edgerton, E. S., Tanner, R. L., Shaw, S. L., et al. (2010). Characterization and quantification of isoprene-derived epoxydiols in ambient aerosol in the southeastern United States. *Environmental Science & Technology*, 44(12), 4590–4596. <https://doi.org/10.1021/Es100596b>
- Claeys, M., Graham, B., Vas, G., Wang, W., Vermeylen, R., Pashynska, V., et al. (2004). Formation of secondary organic aerosols through photooxidation of isoprene. *Science*, 303(5661), 1173–1176. <https://doi.org/10.1126/science.1092805>
- Claeys, M., Wang, W., Ion, A. C., Kourtchev, I., Gelencser, A., & Maenhaut, W. (2004). Formation of secondary organic aerosols from isoprene and its gas-phase oxidation products through reaction with hydrogen peroxide. *Atmospheric Environment*, 38(25), 4093–4098. <https://doi.org/10.1016/j.atmosenv.2004.06.001>
- Cole-Filipiak, N. C., O'Connor, A. E., & Elrod, M. J. (2010). Kinetics of the hydrolysis of atmospherically relevant isoprene-derived hydroxy epoxides. *Environmental Science & Technology*, 44(17), 6718–6723. <https://doi.org/10.1021/es1019228>
- Darer, A. I., Cole-Filipiak, N. C., O'Connor, A. E., & Elrod, M. J. (2011). Formation and stability of atmospherically relevant isoprene-derived organosulfates and organonitrates. *Environmental Science & Technology*, 45(5), 1895–1902. <https://doi.org/10.1021/Es103797z>
- Ding, X., He, Q.-F., Shen, R.-Q., Yu, Q.-Q., & Wang, X.-M. (2014). Spatial distributions of secondary organic aerosols from isoprene, monoterpenes,  $\beta$ -caryophyllene, and aromatics over China during summer. *Journal of Geophysical Research: Atmospheres*, 119, 11,877–11,891. <https://doi.org/10.1002/2014JD021748>
- Ding, X., Wang, X.-M., Gao, B., Fu, X.-X., He, Q.-F., Zhao, X.-Y., et al. (2012). Tracer-based estimation of secondary organic carbon in the Pearl River Delta, South China. *Journal of Geophysical Research*, 117, D05313. <https://doi.org/10.1029/2011JD016596>
- Ding, X., Wang, X. M., Xie, Z. Q., Zhang, Z., & Sun, L. G. (2013). Impacts of Siberian biomass burning on organic aerosols over the North Pacific Ocean and the Arctic: Primary and secondary organic tracers. *Environmental Science & Technology*, 47(7), 3149–3157. <https://doi.org/10.1021/Es3037093>
- Ding, X., Wang, X.-M., & Zheng, M. (2011). The influence of temperature and aerosol acidity on biogenic secondary organic aerosol tracers: Observations at a rural site in the central Pearl River Delta region, South China. *Atmospheric Environment*, 45(6), 1303–1311. <https://doi.org/10.1016/j.atmosenv.2010.11.057>
- Ding, X., Zheng, M., Yu, L. P., Zhang, X. L., Weber, R. J., Yan, B., et al. (2008). Spatial and seasonal trends in biogenic secondary organic aerosol tracers and water-soluble organic carbon in the southeastern United States. *Environmental Science & Technology*, 42(14), 5171–5176. <https://doi.org/10.1021/Es7032636>
- Donahue, N. M., Epstein, S. A., Pandis, S. N., & Robinson, A. L. (2011). A two-dimensional volatility basis set: 1. Organic-aerosol mixing thermodynamics. *Atmospheric Chemistry and Physics*, 11(7), 3303–3318. <https://doi.org/10.5194/acp-11-3303-2011>
- Eddingsaas, N. C., VanderVelde, D. G., & Wennberg, P. O. (2010). Kinetics and products of the acid-catalyzed ring-opening of atmospherically relevant butyl epoxy alcohols. *Journal of Physical Chemistry A*, 114(31), 8106–8113. <https://doi.org/10.1021/Jp103907c>
- El Haddad, I., Marchand, N., Temime-Roussel, B., Wortham, H., Piot, C., Besombes, J. L., et al. (2011). Insights into the secondary fraction of the organic aerosol in a Mediterranean urban area: Marseille. *Atmospheric Chemistry and Physics*, 11(5), 2059–2079. <https://doi.org/10.5194/acp-11-2059-2011>
- Fan, S. J., Fan, Q., Yu, W., Luo, X. Y., Wang, B. M., Song, L. L., & Leong, K. L. (2011). Atmospheric boundary layer characteristics over the Pearl River Delta, China, during the summer of 2006: Measurement and model results. *Atmospheric Chemistry and Physics*, 11(13), 6297–6310. <https://doi.org/10.5194/acp-11-6297-2011>
- Fu, P. Q., Kawamura, K., & Barrie, L. A. (2009). Photochemical and other sources of organic compounds in the Canadian high Arctic aerosol pollution during winter-spring. *Environmental Science & Technology*, 43(2), 286–292. <https://doi.org/10.1021/Es803046q>
- Fu, P. Q., Kawamura, K., & Miura, K. (2011). Molecular characterization of marine organic aerosols collected during a round-the-world cruise. *Journal of Geophysical Research*, 116, D13302. <https://doi.org/10.1029/2011JD015604>

- Fu, X., Guo, H., Wang, X., Ding, X., He, Q., Liu, T., & Zhang, Z. (2015). PM<sub>2.5</sub> acidity at a background site in the Pearl River Delta region in fall-winter of 2007–2012. *Journal of Hazardous Materials*, 286(0), 484–492. <https://doi.org/10.1016/j.jhazmat.2015.01.022>
- Fu, X., Wang, X., Guo, H., Cheung, K., Ding, X., Zhao, X., et al. (2014). Trends of ambient fine particles and major chemical components in the Pearl River Delta region: Observation at a regional background site in fall and winter. *Science of the Total Environment*, 497–498, 274–281. <https://doi.org/10.1016/j.scitotenv.2014.08.008>
- Gaston, C. J., Riedel, T. P., Zhang, Z., Gold, A., Surratt, J. D., & Thornton, J. A. (2014). Reactive uptake of an isoprene-derived epoxydiol to submicron aerosol particles. *Environmental Science & Technology*, 48(19), 11,178–11,186. <https://doi.org/10.1021/es5034266>
- Gu, D., Wang, Y., Smeltzer, C., & Liu, Z. (2013). Reduction in NO<sub>x</sub> emission trends over China: Regional and seasonal variations. *Environmental Science & Technology*, 47(22), 12,912–12,919. <https://doi.org/10.1021/es401727e>
- Guenther, A., Karl, T., Harley, P., Wiedinmyer, C., Palmer, P. I., & Geron, C. (2006). Estimates of global terrestrial isoprene emissions using MEGAN (model of emissions of gases and aerosols from nature). *Atmospheric Chemistry and Physics*, 6, 3181–3210. <https://doi.org/10.5194/acp-6-3181-2006>
- Guo, H., Xu, L., Bougiatioti, A., Cerully, K. M., Capps, S. L., Hite, J. R., et al. (2015). Fine-particle water and pH in the southeastern United States. *Atmospheric Chemistry and Physics*, 15(9), 5211–5228. <https://doi.org/10.5194/acp-15-5211-2015>
- He, Q.-F., Ding, X., Wang, X.-M., Yu, J.-Z., Fu, X.-X., Liu, T.-Y., et al. (2014). Organosulfates from pinene and isoprene over the Pearl River Delta, South China: Seasonal variation and implication in formation mechanisms. *Environmental Science & Technology*, 48(16), 9236–9245. <https://doi.org/10.1021/es501299v>
- Heald, C. L., Henze, D. K., Horowitz, L. W., Feddema, J., Lamarque, J. F., Guenther, A., et al. (2008). Predicted change in global secondary organic aerosol concentrations in response to future climate, emissions, and land use change. *Journal of Geophysical Research*, 113, D05211. <https://doi.org/10.1029/2007JD009092>
- Hennigan, C. J., Izumi, J., Sullivan, A. P., Weber, R. J., & Nenes, A. (2015). A critical evaluation of proxy methods used to estimate the acidity of atmospheric particles. *Atmospheric Chemistry and Physics*, 15(5), 2775–2790. <https://doi.org/10.5194/acp-15-2775-2015>
- Hofzumahaus, A., Rohrer, F., Lu, K. D., Bohn, B., Brauers, T., Chang, C. C., et al. (2009). Amplified trace gas removal in the troposphere. *Science*, 324(5935), 1702–1704. <https://doi.org/10.1126/science.1164566>
- Hu, W. W., Campuzano-Jost, P., Palm, B. B., Day, D. A., Ortega, A. M., Hayes, P. L., et al. (2015). Characterization of a real-time tracer for isoprene epoxydiols-derived secondary organic aerosol (IEPOX-SOA) from aerosol mass spectrometer measurements. *Atmospheric Chemistry and Physics*, 15(20), 11,807–11,833. <https://doi.org/10.5194/acp-15-11807-2015>
- Huang, X. F., Hu, M., He, L. Y., & Tang, X. Y. (2005). Chemical characterization of water-soluble organic acids in PM<sub>2.5</sub> in Beijing, China. *Atmospheric Environment*, 39(16), 2819–2827. <https://doi.org/10.1016/j.atmosenv.2004.08.038>
- Ion, A. C., Vermeylen, R., Kourtchev, I., Cafmeyer, J., Chi, X., Gelencser, A., et al. (2005). Polar organic compounds in rural PM (2.5) aerosols from K-puszta, Hungary, during a 2003 summer field campaign: Sources and diel variations. *Atmospheric Chemistry and Physics*, 5, 1805–1814. <https://doi.org/10.5194/acp-5-1805-2005>
- Jacobs, M. I., Darer, A. I., & Elrod, M. J. (2013). Rate constants and products of the OH reaction with isoprene-derived epoxides. *Environmental Science & Technology*, 47(22), 12,868–12,876. <https://doi.org/10.1021/es403340g>
- Jang, M., Czoschke, N. M., Lee, S., & Kamens, R. M. (2002). Heterogeneous atmospheric aerosol production by acid-catalyzed particle-phase reactions. *Science*, 298(5594), 814–817. <https://doi.org/10.1126/science.1075798>
- Kleindienst, T. E., Jaoui, M., Lewandowski, M., Offenberg, J. H., Lewis, C. W., Bhawe, P. V., & Edney, E. O. (2007). Estimates of the contributions of biogenic and anthropogenic hydrocarbons to secondary organic aerosol at a southeastern US location. *Atmospheric Environment*, 41(37), 8288–8300. <https://doi.org/10.1016/j.atmosenv.2007.06.045>
- Kleindienst, T. E., Lewandowski, M., Offenberg, J. H., Edney, E. O., Jaoui, M., Zheng, M., et al. (2010). Contribution of primary and secondary sources to organic aerosol and PM<sub>2.5</sub> at SEARCH network sites. *Journal of the Air & Waste Management Association*, 60(11), 1388–1399. <https://doi.org/10.3155/1047-3289.60.11.1388>
- Kourtchev, I., Ruuskanen, T., Maenhaut, W., Kulmala, M., & Claeys, M. (2005). Observation of 2-methyltetrols and related photo-oxidation products of isoprene in boreal forest aerosols from Hyttälä, Finland. *Atmospheric Chemistry and Physics*, 5(10), 2761–2770. <https://doi.org/10.5194/acp-5-2761-2005>
- Kristensson, K., & Glasius, M. (2011). Organosulfates and oxidation products from biogenic hydrocarbons in fine aerosols from a forest in North West Europe during spring. *Atmospheric Environment*, 45(27), 4546–4556. <https://doi.org/10.1016/j.atmosenv.2011.05.063>
- Kroll, J. H., Ng, N. L., Murphy, S. M., Flagan, R. C., & Seinfeld, J. H. (2005). Secondary organic aerosol formation from isoprene photooxidation under high-NO<sub>x</sub> conditions. *Geophysical Research Letters*, 32, L18808. <https://doi.org/10.1029/2005GL023637>
- Kroll, J. H., Ng, N. L., Murphy, S. M., Flagan, R. C., & Seinfeld, J. H. (2006). Secondary organic aerosol formation from isoprene photooxidation. *Environmental Science & Technology*, 40(6), 1869–1877. <https://doi.org/10.1021/Es0524301>
- Kroll, J. H., & Seinfeld, J. H. (2008). Chemistry of secondary organic aerosol: Formation and evolution of low-volatility organics in the atmosphere. *Atmospheric Environment*, 42(16), 3593–3624. <https://doi.org/10.1016/j.atmosenv.2008.01.003>
- Lee, Y. C., Shindell, D. T., Faluvegi, G., Wenig, M., Lam, Y. F., Ning, Z., et al. (2014). Increase of ozone concentrations, its temperature sensitivity and the precursor factor in South China. *Tellus Series B: Chemical and Physical Meteorology*, 66. <https://doi.org/10.3402/Tellusb.V66.23455>
- Lewandowski, M., Piletic, I. R., Kleindienst, T. E., Offenberg, J. H., Beaver, M. R., Jaoui, M., et al. (2013). Secondary organic aerosol characterization at field sites across the United States during the spring-summer period. *International Journal of Environmental Analytical Chemistry*, 93(10), 1084–1103. <https://doi.org/10.1080/03067319.2013.803545>
- Lin, Y. H., Knipping, E. M., Edgerton, E. S., Shaw, S. L., & Surratt, J. D. (2013). Investigating the influences of SO<sub>2</sub> and NH<sub>3</sub> levels on isoprene-derived secondary organic aerosol formation using conditional sampling approaches. *Atmospheric Chemistry and Physics*, 13(16), 8457–8470. <https://doi.org/10.5194/acp-13-8457-2013>
- Lin, Y.-H., Zhang, H., Pye, H. O. T., Zhang, Z., Marth, W. J., Park, S., et al. (2013). Epoxide as a precursor to secondary organic aerosol formation from isoprene photooxidation in the presence of nitrogen oxides. *Proceedings of the National Academy of Sciences of the United States of America*, 110(17), 6718–6723. <https://doi.org/10.1073/pnas.1221150110>
- Lin, Y. H., Zhang, Z. F., Docherty, K. S., Zhang, H. F., Budisulistiorini, S. H., Rubitschun, C. L., et al. (2012). Isoprene epoxydiols as precursors to secondary organic aerosol formation: Acid-catalyzed reactive uptake studies with authentic compounds. *Environmental Science & Technology*, 46(1), 250–258. <https://doi.org/10.1021/Es202554c>
- Liu, J., L. E., D'Ambro, B. H., Lee, F. D., Lopez-Hilfiker, R. A., Zaveri, J. C., et al. (2016). Efficient isoprene secondary organic aerosol formation from a non-IEPOX pathway. *Environmental Science & Technology*, 50(18), 9872–9880. <https://doi.org/10.1021/acs.est.6b01872>
- Liu, J., Russell, L. M., Lee, A. K. Y., McKinney, K. A., Surratt, J. D., & Ziemann, P. J. (2017). Observational evidence for pollution-influenced selective uptake contributing to biogenic secondary organic aerosols in the southeastern U. S. *Geophysical Research Letters*, 44, 8056–8064. <https://doi.org/10.1002/2017GL074665>



- Liu, J., Zhang, X., Parker, E. T., Veres, P. R., Roberts, J. M., de Gouw, J. A., et al. (2012). On the gas-particle partitioning of soluble organic aerosol in two urban atmospheres with contrasting emissions: 2. Gas and particle phase formic acid. *Journal of Geophysical Research*, *117*, D00V21. <https://doi.org/10.1029/2012JD017912>
- Lopez-Hilfiker, F. D., Mohr, C., L. E., D'Ambro, A., Lutz, T. P., Riedel, C. J., et al. (2016). Molecular composition and volatility of organic aerosol in the southeastern U.S.: Implications for IEPOX derived SOA. *Environmental Science & Technology*, *50*(5), 2200–2209. <https://doi.org/10.1021/acs.est.5b04769>
- Lu, K. D., Hofzumahaus, A., Holland, F., Bohn, B., Brauers, T., Fuchs, H., et al. (2013). Missing OH source in a suburban environment near Beijing: Observed and modelled OH and HO<sub>2</sub> concentrations in summer 2006. *Atmospheric Chemistry and Physics*, *13*(2), 1057–1080. <https://doi.org/10.5194/acp-13-1057-2013>
- Marais, E. A., Jacob, D. J., Jimenez, J. L., Campuzano-Jost, P., Day, D. A., Hu, W., et al. (2016). Aqueous-phase mechanism for secondary organic aerosol formation from isoprene: Application to the southeast United States and co-benefit of SO<sub>2</sub> emission controls. *Atmospheric Chemistry and Physics*, *16*(3), 1603–1618. <https://doi.org/10.5194/acp-16-1603-2016>
- McNeill, V. F. (2015). Aqueous organic chemistry in the atmosphere: Sources and chemical processing of organic aerosols. *Environmental Science & Technology*, *49*(3), 1237–1244. <https://doi.org/10.1021/es5043707>
- Minerath, E. C., Schultz, M. P., & Elrod, M. J. (2009). Kinetics of the reactions of isoprene-derived epoxides in model tropospheric aerosol solutions. *Environmental Science & Technology*, *43*(21), 8133–8139. <https://doi.org/10.1021/es902304p>
- Nan, J., Wang, S., Guo, Y., Xiang, Y., & Zhou, B. (2017). Study on the daytime OH radical and implication for its relationship with fine particles over megacity of Shanghai, China. *Atmospheric Environment*, *154*, 167–178. <https://doi.org/10.1016/j.atmosenv.2017.01.046>
- Nenes, A., Pandis, S. N., & Pilinis, C. (1998). ISORROPIA: A new thermodynamic equilibrium model for multiphase multicomponent inorganic aerosols. *Aquatic Geochemistry*, *4*(1), 123–152. <https://doi.org/10.1023/A:1009604003981>
- Ng, N. L., Kwan, A. J., Surratt, J. D., Chan, A. W. H., Chhabra, P. S., Sorooshian, A., et al. (2008). Secondary organic aerosol (SOA) formation from reaction of isoprene with nitrate radicals (NO<sub>3</sub>). *Atmospheric Chemistry and Physics*, *8*(14), 4117–4140. <https://doi.org/10.5194/acp-8-4117-2008>
- Nguyen, T. B., Bates, K. H., Crouse, J. D., Schwantes, R. H., Zhang, X., Kjaergaard, H. G., et al. (2015). Mechanism of the hydroxyl radical oxidation of methacryloyl peroxyxynitrate (MPAN) and its pathway toward secondary organic aerosol formation in the atmosphere. *Physical Chemistry Chemical Physics (PCCP)*, *17*(27), 17,914–17,926. <https://doi.org/10.1039/c5cp02001h>
- Nguyen, T. B., Coggon, M. M., Bates, K. H., Zhang, X., Schwantes, R. H., Schilling, K. A., et al. (2014). Organic aerosol formation from the reactive uptake of isoprene epoxydiols (IEPOX) onto non-acidified inorganic seeds. *Atmospheric Chemistry and Physics*, *14*(7), 3497–3510. <https://doi.org/10.5194/acp-14-3497-2014>
- Nguyen, T. B., Crouse, J. D., Teng, A. P., St, J. M., Clair, F., Paulot, G. M. W., & Wennberg, P. O. (2015). Rapid deposition of oxidized biogenic compounds to a temperate forest. *Proceedings of the National Academy of Sciences of the United States of America*, *112*(5), E392–E401. <https://doi.org/10.1073/pnas.1418702112>
- NIOSH (1999). Method 5040 issue 3 (Interim): Elemental carbon (diesel exhaust). In *NIOSH manual of analytical methods*. Cincinnati, OH: National Institute of Occupational Safety and Health. Retrieved from Available at <http://www.cdc.gov/niosh/docs/2003-154/pdfs/5040.pdf>
- Paulot, F., Crouse, J. D., Kjaergaard, H. G., Kroll, J. H., Seinfeld, J. H., & Wennberg, P. O. (2009). Isoprene photooxidation: New insights into the production of acids and organic nitrates. *Atmospheric Chemistry and Physics*, *9*(4), 1479–1501. <https://doi.org/10.5194/acp-9-1479-2009>
- Paulot, F., Crouse, J. D., Kjaergaard, H. G., Kürten, A., St, J. M., Clair, J. H. S., & Wennberg, P. O. (2009). Unexpected epoxide formation in the gas-phase photooxidation of isoprene. *Science*, *325*(5941), 730–733. <https://doi.org/10.1126/science.1172910>
- Pye, H. O. T., Pinder, R. W., Piletic, I. R., Xie, Y., Capps, S. L., Lin, Y.-H., et al. (2013). Epoxide pathways improve model predictions of isoprene markers and reveal key role of acidity in aerosol formation. *Environmental Science & Technology*, *47*(19), 11,056–11,064. <https://doi.org/10.1021/es402106h>
- Rattanavaraha, W., Chu, K., Budisulistiorini, H., Riva, M., Lin, Y. H., Edgerton, E. S., et al. (2016). Assessing the impact of anthropogenic pollution on isoprene-derived secondary organic aerosol formation in PM<sub>2.5</sub> collected from the Birmingham, Alabama, ground site during the 2013 Southern Oxidant and Aerosol Study. *Atmospheric Chemistry and Physics*, *16*(8), 4897–4914. <https://doi.org/10.5194/acp-16-4897-2016>
- Riedel, T. P., Lin, Y.-H., Budisulistiorini, S. H., Gaston, C. J., Thornton, J. A., Zhang, Z., et al. (2015). Heterogeneous reactions of isoprene-derived epoxides: Reaction probabilities and molar secondary organic aerosol yield estimates. *Environmental Science & Technology Letters*, *2*(2), 38–42. <https://doi.org/10.1021/ez500406f>
- Riedel, T. P., Lin, Y. H., Zhang, Z., Chu, K., Thornton, J. A., Vizuete, W., et al. (2016). Constraining condensed-phase formation kinetics of secondary organic aerosol components from isoprene epoxydiols. *Atmospheric Chemistry and Physics*, *16*(3), 1245–1254. <https://doi.org/10.5194/acp-16-1245-2016>
- Riva, M., Budisulistiorini, S. H., Chen, Y., Zhang, Z., D'Ambro, E. L., Zhang, X., et al. (2016). Chemical characterization of secondary organic aerosol from oxidation of isoprene hydroxyhydroperoxides. *Environmental Science & Technology*, *50*(18), 9889–9899. <https://doi.org/10.1021/acs.est.6b02511>
- Riva, M., Budisulistiorini, S. H., Zhang, Z., Gold, A., & Surratt, J. D. (2016). Chemical characterization of secondary organic aerosol constituents from isoprene ozonolysis in the presence of acidic aerosol. *Atmospheric Environment*, *130*(Supplement C), 5–13. <https://doi.org/10.1016/j.atmosenv.2015.06.027>
- Seinfeld, J. H., & Pankow, J. F. (2003). Organic atmospheric particulate material. *Annual Review of Physical Chemistry*, *54*, 121–140. <https://doi.org/10.1146/annurev.physchem.54.011002.103756>
- Speer, R. E., Edney, E. O., & Kleindienst, T. E. (2003). Impact of organic compounds on the concentrations of liquid water in ambient PM<sub>2.5</sub>. *Journal of Aerosol Science*, *34*(1), 63–77. [https://doi.org/10.1016/S0021-8502\(02\)00152-0](https://doi.org/10.1016/S0021-8502(02)00152-0)
- St. Clair, J. M., Rivera-Rios, J. C., Crouse, J. D., Knap, H. C., Bates, K. H., Teng, A. P., et al. (2016). Kinetics and products of the reaction of the first-generation isoprene hydroxy hydroperoxide (ISOPOOH) with OH. *The Journal of Physical Chemistry A*, *120*(9), 1441–1451. <https://doi.org/10.1021/acs.jpca.5b06532>
- Stone, E. A., Nguyen, T. T., Pradhan, B. B., & Man Dangol, P. (2012). Assessment of biogenic secondary organic aerosol in the Himalayas. *Environmental Chemistry*, *9*(3), 263. <https://doi.org/10.1071/EN12002>
- Surratt, J. D., Chan, A. W. H., Eddingsaas, N. C., Chan, M., Loza, C. L., Kwan, A. J., et al. (2010). Reactive intermediates revealed in secondary organic aerosol formation from isoprene. *Proceedings of the National Academy of Sciences of the United States of America*, *107*(15), 6640–6645. <https://doi.org/10.1073/pnas.0911114107>
- Surratt, J. D., Lewandowski, M., Offenberg, J. H., Jaoui, M., Kleindienst, T. E., Edney, E. O., & Seinfeld, J. H. (2007). Effect of acidity on secondary organic aerosol formation from isoprene. *Environmental Science & Technology*, *41*(15), 5363–5369. <https://doi.org/10.1021/Es0704176>



- Surratt, J. D., Murphy, S. M., Kroll, J. H., Ng, N. L., Hildebrandt, L., Sorooshian, A., et al. (2006). Chemical composition of secondary organic aerosol formed from the photooxidation of isoprene. *Journal of Physical Chemistry A*, *110*(31), 9665–9690. <https://doi.org/10.1021/Jp061734m>
- Wang, X. M., Situ, S. P., Guenther, A., Chen, F., Wu, Z. Y., Xia, B. C., & Wang, T. J. (2011). Spatiotemporal variability of biogenic terpenoid emissions in Pearl River Delta, China, with high-resolution land-cover and meteorological data. *Tellus Series B: Chemical and Physical Meteorology*, *63*(2), 241–254. <https://doi.org/10.1111/j.1600-0889.2010.00523.x>
- Wang, Y., Ren, J., Huang, X. H. H., Tong, R., & Yu, J. Z. (2017). Synthesis of four monoterpene-derived organosulfates and their quantification in atmospheric aerosol samples. *Environmental Science & Technology*, *51*(12), 6791–6801. <https://doi.org/10.1021/acs.est.7b01179>
- Whalley, L., Stone, D., & Heard, D. (2014). New insights into the tropospheric oxidation of isoprene: Combining field measurements, laboratory studies, chemical modelling and quantum theory. *Atmospheric and Aerosol Chemistry*, *339*, 55–95. [https://doi.org/10.1007/128\\_2012\\_359](https://doi.org/10.1007/128_2012_359)
- Worton, D. R., Goldstein, A. H., Farmer, D. K., Docherty, K. S., Jimenez, J. L., Gilman, J. B., et al. (2011). Origins and composition of fine atmospheric carbonaceous aerosol in the Sierra Nevada Mountains, California. *Atmospheric Chemistry and Physics*, *11*(19), 10,219–10,241. <https://doi.org/10.5194/acp-11-10219-2011>
- Worton, D. R., Surratt, J. D., LaFranchi, B. W., Chan, A. W. H., Zhao, Y., Weber, R. J., et al. (2013). Observational insights into aerosol formation from isoprene. *Environmental Science & Technology*, *47*(20), 11,403–11,413. <https://doi.org/10.1021/es4011064>
- Xu, L., Guo, H., Boyd, C. M., Klein, M., Bougiatioti, A., Cerully, K. M., et al. (2015). Effects of anthropogenic emissions on aerosol formation from isoprene and monoterpenes in the southeastern United States. *Proceedings of the National Academy of Sciences of the United States of America*, *112*(1), 37–42. <https://doi.org/10.1073/pnas.1417609112>
- Xu, L., Middlebrook, A. M., Liao, J., de Gouw, J. A., Guo, H., Weber, R. J., et al. (2016). Enhanced formation of isoprene-derived organic aerosol in sulfur-rich power plant plumes during southeast Nexus. *Journal of Geophysical Research: Atmospheres*, *121*, 11,137–11,153. <https://doi.org/10.1002/2016JD025156>
- Yao, X. H., Fang, M., Chan, C. K., Ho, K. F., & Lee, S. C. (2004). Characterization of dicarboxylic acids in PM<sub>2.5</sub> in Hong Kong. *Atmospheric Environment*, *38*(7), 963–970. <https://doi.org/10.1016/j.atmosenv.2003.10.048>
- Zhang, Y., Chen, Y., Lambe, A. T., Olson, N. E., Lei, Z., Craig, R. L., et al. (2018). Effect of the aerosol-phase state on secondary organic aerosol formation from the reactive uptake of isoprene-derived epoxydiols (IEPOX). *Environmental Science & Technology Letters*, *5*(3), 167–174. <https://doi.org/10.1021/acs.estlett.8b00044>
- Zheng, J. Y., Zheng, Z. Y., Yu, Y. F., & Zhong, L. J. (2010). Temporal, spatial characteristics and uncertainty of biogenic VOC emissions in the Pearl River Delta region, China. *Atmospheric Environment*, *44*(16), 1960–1969. <https://doi.org/10.1016/j.atmosenv.2010.03.001>